Methods

Wild radish experiments.

We used *R. raphanistrum* seeds from a second generation of untreated greenhouse-grown plants. We germinated about 10 seeds from each of 13 maternal families in a greenhouse. At the four-leaf stage, each plant was randomly assigned to one of the two treatments (3–5 plants per treatment per family). The caterpillar herbivory treatment was maintained throughout the growth of the plant. Effects of herbivory on seed set are reported elsewhere[19]. Seeds from 8 of the original 13 families were chosen for the transgenerational experiment because they spanned the range of tolerance to herbivory[19], and 2–4 seeds from each of 58 maternal plants within 8 grandmaternal families (a total of 126 plants) were grown in a greenhouse and inoculated with a single newly hatched *P. rapae* larva. Caterpillars were not caged. After four days, the caterpillars were weighed.

Effects of grandmaternal family (fixed), maternal environment (control or herbivory; fixed), maternal family (nested within grandmaternal family by treatment interaction; random) and seed mass (covariate) on caterpillar growth were analysed using a mixed-model analysis of variance (ANOVA). *F*-ratios for grandmaternal family and treatment effects were calculated with maternal family nested in grandmaternal family by treatment interaction mean-square and degrees of freedom in the denominator.

For phytochemical analysis, glucosinolates were analysed using modified procedures for determination of trimethylsilyl glucosinolate derivatives with capillary gas chromatography and flame ionization detection[20]. Seed nitrogen and carbon were determined from a separate set of seeds using dynamic flash-combustion and gas-chromatographic separation and a thermal-conductivity detection system (Division of Agriculture and Nature Resources, University of California, Davis).

Daphnia experiments.

We used a *Daphnia cucullata* clone isolated from Thaler lake, Germany. The experiments were conducted in the laboratory under constant conditions at 20 °C and fluorescent light in a synthetic medium. The F_0 generation had been synchronized by always raising the third brood offspring born within 12 h, starting from a single *Daphnia*. *Daphnia* were fed *ad libitum* daily with *Scenedesumus acutus* ($1.5\ mg\ C\ l^{-1}$).

Animals with freshly deposited eggs were placed into 0.75 l medium containing a 125-μm net cage, enclosing either 10 fourth-instar larvae of *Chaoborus flavicans* or 4 *Leptodora kindtii*, or no predators for controls. The net cages prevented direct contact between predators and prey.

Predation experiments with *Chaoborus* were conducted for 0.5 h with each prey morph separately in 100 ml medium with 10 prey organisms and a single predator. Predation trials with *Leptodora* were conducted with 10 prey organisms of each morph together in 0.5 l in 24-h experiments. In each experiment, animals of the same age and body size class (0.6–0.8 mm, from the eye to the base of the tail spine) but of different morphology were compared.

We induced helmet formation in *Daphnia* by using *Chaoborus* kairomones. We placed four *Chaoborus* larvae in net cages in 1.5-l beakers and changed the water ever day. Chaoborids were fed daily with 10–15 prey (*D. cucullata* and *Ceriodaphnia* sp.). The F_0 generation had been born and raised in these beakers in either the control or kairomone treatment. We used three beakers per treatment as replicates, which did not differ and were pooled for analysis.

Daphnids were measured with a digital image-analysis system (SIS, Münster, Germany). To compensate for small changes in body length within an age class, we calculated the relative helmet length (helmet length/body length × 100). Relative helmet length is a good predictor of the defensive effect within an age class. The relative values were arcsin-transformed for analysis. In the induction treatment, differences between control and kairomone treatment were compared using *t*-tests. Effects of induced *Daphnia* phenotypes on predation were analysed by using a Mann–Whitney-*U*-test for *Chaoborus* and with a paired Wilcoxon test for related samples for *Leptodora*. To test for transgenerational effects, we compared the treatments within each brood and age class (Table 2, Fig. 3) with ANOVA and Bonferroni adjustments.

Received 29 March; accepted 28 June 1999.

1. Thompson, J. N. Rapid evolution as an ecological process. *Trends Ecol. Evol.* **13,** 329–332 (1998).
2. Seeley, R. H. Intense natural selection caused a rapid morphological transition in a living marine snail [*Littorina obtusata*]. *Proc. Natl Acad. Sci. USA* **83,** 6897–6901 (1986).
3. Magurran, A. E., Seghers, B. H., Carvalho, G. R. & Shaw, P. W. Behavioural consequences of an artificial introduction of guppies (*Poecilia reticulata*) in N. Trinidad: Evidence for the evolution of anti-predator behaviour in the wild. *Proc. R. Soc. Lond. B* **248,** 117–122 (1992).
4. Reznick, D. N., Shaw, F. H. Rodd, F. H. & Shaw, R. G. Evaluation of the rate of evolution in natural populations of guppies (*Poecilia reticulata*). *Science* **275,** 1934–1937 (1997).
5. Lenski, R. E. & Levin, B. R. Constraints on the coevolution of bacteria and virulent phage: A model, some experiments, and predictions for natural communities. *Am. Nat.* **125,** 585–602 (1985).
6. Thompson, J. N. & Burdon, J. J. Gene-for-gene coevolution between plants and parasites. *Nature* **360,** 121–125 (1992).
7. Frita, R. S. & Simms, E. L. (eds) *Plant Resistance to Herbivores and Pathogens* (Univ. Chicago Press, 1992).
8. Tollrian, R. & Harvell, C. D. (eds) *The Ecology and Evolution of Inducible Defenses* (Princeton Univ. Press, Princeton, NJ, 1999).
9. Agrawal, A. A., Tuzun, S. & Bent, E. (eds) *Induced Plant Defense against Pathogens and Herbivores: Biochemistry, Ecology, and Agriculture* (American Phytopathological Society Press, St Paul, Minnesota, in the press).
10. Karban, R. & Baldwin, I. T. *Induced Responses to Herbivory* (Univ. Chicago Press, 1997).
11. Agrawal, A. A. Induced responses to herbivory and increased plant performance. *Science* **279,** 1201–1202 (1998).
12. Mousseau, T. A. & Fox, C. W. (eds) *Maternal Effects as Adaptations* (Oxford Univ. Press, New York, 1998).
13. Rossiter, M. Incidence and consequences of inherited environmental effects. *Annu. Rev. Ecol. Syst.* **27,** 451–476 (1996).
14. Roach, D. A. & Wulff, R. D. Maternal effects in plants. *Annu. Rev. Ecol. Syst.* **18,** 209–236 (1987).
15. Schmitt, J., Niles, J. & Wulff, R. D. Norms of reaction of seed traits to maternal environments in *Plantago lanceolata*. *Am. Nat.* **139,** 451–466 (1992).
16. Tollrian, R. Predator-induced morphological defenses: Costs, life history shifts, and maternal effects in *Daphnia pulex*. *Ecology* **76,** 1691–1705 (1995).
17. Fox, C. W., Thakar, M. S. & Mousseau, T. A. Egg size plasticity in a seed beetle: An adaptive maternal effect. *Am. Nat.* **149,** 149–163 (1997).
18. Thiede, D. A. Maternal inheritance and its effect on adaptive evolution: A quantitative genetic analysis of maternal effects in a natural plant population. *Evolution* **52,** 998–1015 (1998).
19. Agrawal, A. A. Induced responses to herbivory in wild radish: Effects on several herbivores and plant fitness. *Ecology* **80,** 1713–1723 (1999).
20. Agrawal, A. A., Strauss, S. Y. & Stout, M. J. Costs of induced responses and tolerance to herbivory in male and female fitness components of wild radish. *Evolution* (in the press).
21. Hutchinson, G. E. *A Treatise on Limnology* Vol. 2 (Wiley, New York, 1967).
22. Jacobs, J. in *Daphnia* (eds Peters, R. H. & de Bernardi, R.) 325–252 (Memorie dell'Istituto Italiano di Idrobiologia Dott, Verbania Palanza, 1987).
23. Tollrian, R. Predator-induced helmet formation in *Daphnia cucullata* (Sars). *Arch. Hydrobiol.* **119,** 191–196 (1990).
24. Tolliran, R. & Von Elert, E. Enrichment and purification of *Chaoborus* kairomone from water: Further steps toward its chemical characterization. *Limnol. Oceanogr.* **39,** 788–796 (1994).
25. Schluter, D. & Gustafsson, L. Maternal inheritance of condition and clutch size in the collared flycatcher. *Evolution* **47,** 658–667 (1993).
26. Lenski, R. E. *et al.* Epistatic effects of promoter and repressor functions of the Tn10 tetracycline-resistance operon on the fitness of *Escherichia coli*. *Mol. Ecol.* **3,** 127–135 (1994).
27. Stanton, M. L. Seed variation in wild radish: Effect of seed on components of seedling and adult fitness. *Ecology* **65,** 1105–1112 (1984).
28. Gilbert, J. J. Rotifer ecology and embryological induction. *Science* **151,** 1234–1237 (1966).
29. Roberts, D. A. Acquired resistance to Tobacco Mosaic Virus transmitted to the progeny of hypersensitive tobacco. *Virology* **124,** 161–163 (1983).
30. Shine, R. & Downes, S. J. Can pregnant lizards adjust their offspring phenotypes to environmental conditions? *Oecologia* **119,** 1–8 (1999).

Acknowledgements

We thank R. Karban, the plant-herbivore group at Davis and W. Gabriel for advice and encouragement; M. Morra and V. Borek for help with phytochemical analyses; R. J. Mercader, M. Kredler, S. Y. Strauss, J. Kniskern and E. Hochmuth for help with experiments; and L. S. Adler, S. Diehl, H. Dingle, R. Karban, R. E. Lenski, T. W. Schoener, S. Y. Strauss, J. S. Thaler, D. A. Thiede, and T. G. Whitham for comments on the manuscript. This work was supported by the US NSF.

Correspondence and requests for materials should be addressed to A.A.A. (e-mail: aaagrawal@ucdavis. edu) or R.T. (e-mail: Ralph.Tollrian@lrz.uni-muenchen.de).

Genetic enhancement of learning and memory in mice

Ya-Ping Tang*, Eiji Shimizu*, Gilles R. Dube†, Claire Rampon*, Geoffrey A. Kerchner‡, Min Zhuo‡, Guosong Liu† & Joe Z. Tsien*

* *Department of Molecular Biology, Princeton University, Princeton, New Jersey 08544-1014, USA*
† *Department of Brain and Cognitive Science, The Center for Learning and Memory, MIT, Cambridge, Massachusetts 02139, USA*
‡ *Departments of Anesthesiology and Neurobiology, School of Medicine, Washington University, St Louis, Missouri 63110, USA*

Hebb's rule (1949) states that learning and memory are based on modifications of synaptic strength among neurons that are simultaneously active. This implies that enhanced synaptic coincidence detection would lead to better learning and memory. If the NMDA (*N*-methyl-D-aspartate) receptor, a synaptic coincidence detector[1–4], acts as a graded switch for memory formation, enhanced signal detection by NMDA receptors should enhance learning and memory. Here we show that overexpression of NMDA receptor 2B (NR2B) in the forebrains of transgenic mice leads to enhanced activation of NMDA receptors, facilitating synaptic potentiation in response to stimulation at 10–100 Hz. These mice exhibit superior ability in learning and memory in various behavioural tasks, showing that NR2B is critical in gating the age-dependent threshold for plasticity and memory formation. NMDA-receptor-dependent modifications of synaptic

efficacy, therefore, represent a unifying mechanism for associative learning and memory. Our results suggest that genetic enhancement of mental and cognitive attributes such as intelligence and memory in mammals is feasible.

The NMDA receptors are heteromeric complexes consisting of subunit 1 (NR1) and various NR2 subunits[5,6]. The NR1 subunit is essential for channel function, whereas the NR2 subunit regulates channel gating and Mg^{2+} dependency[7]. In adult forebrain regions such as the hippocampus and cortex, only NR2A and NR2B subunits are available to form the receptor complex with NR1 subunit. The recombinant NR1–NR2B complex *in vitro* shows longer excitatory postsynaptic potentials (EPSPs) than does the NRI–NR2A complex[8]. Increased incorporation of NR2B into the receptor complex *in vivo* should allow the NMDA receptors to increase the time window for detecting synaptic coincidence. NR2B expression is downregulated during the transition from juvenile to adult[9,10], correlating with the gradual shortening of the EPSP duration of the NMDA channel[11,12]. This could decrease NMDA-mediated plasticity, and perhaps explain decreased memory performance in adult animals including songbirds, monkeys and humans[13,14].

To test whether the NR2B subunit is crucial for implementing Hebb's rule and gating synaptic plasticity and memory, we overexpressed the NR2B subunit postnatally in the mouse forebrain using the CaM-kinase-II promoter[15,16] (Fig. 1a). Of seven lines produced, we report here results from two independent lines (Tg-1 and Tg-2) that we have systematically analysed. They show similar expression patterns and levels of NR2B, and nearly identical electrophysiological and behavioural phenotypes.

These transgenic animals, named *Doogie*, show normal growth and body weights and mate normally. Their open-field behaviour is indistinguishable from that of wild-type littermates, and we observed no seizure or convulsion in transgenic animals. As our northern blot analysis indicates, NR2B transgene expression is enriched in the cortex and hippocampus, with little expression in the thalamus, brainstem and cerebellum (Fig. 1b). Western blot analysis showed about twice as much NR2B protein in the cortex and hippocampus of transgenic mice as in the wild type (Fig. 1c). There is also a slight increase in NR1 protein, but no change in NR2A expression in these regions (Fig. 1c). This indicates that both the ratio of NR2B to NR2A in the receptor complex and the total number of NMDA receptors may be increased. We investigated the transgene's anatomical distribution using *in situ* hybridization and found that the transgene was highly enriched in the cortex, striatum, hippocampus and amygdala (Fig. 1d). Light microscopy showed no gross structural abnormalities in the transgenic animals (Fig. 1e, f). The shapes and architecture of dendritic spins in the hippocampus and cortex are also normal (Fig. 1g).

To evaluate the elementary properties of the NMDA receptors in single synapses, we used a single-bouton recording technique[17]. Using FM 1-43 dye to label functional synaptic sites in cultured hippocampal neurons, we positioned the tip of an iontophoretic electrode containing 150 mM glutamate next to a relatively isolated synapse (Fig. 2a) and applied glutamate to determine the functional properties of glutamate receptors located in that synapse. Glutamate-evoked responses consisted of either AMPA (α-amino-3-hydroxy-5-methyl-4-isoxazole propionic acid) current alone or both AMPA and NMDA currents, depending on the cell potential. The NMDA component was identified by its 'J'-shaped current–voltage relationship and long decay time (Fig. 2b). NMDA currents were isolated by clamping the cells to +40 mV to remove the voltage-dependent Mg^{2+} block. Initial experiments were carried out with 5 μM DNQX in the bath solution to block AMPA receptors, but we subsequently omitted the antagonist because NMDA current could clearly be isolated from AMPA current based on their respective time courses. All the experiments were conducted in blind fashion.

We first determined the glutamate dose–response curve of the synaptic NMDA receptors (an index of the glutamate affinity of the NMDA receptor) and its voltage-dependent Mg^{2+} block, and found no difference between the two groups of mice (data not shown). As the recombinant NR2B subunit determines the decay phase of NMDA currents *in vitro*[8], we next measured the NMDA-channel decay time for currents evoked by a saturating dose of glutamate (100 nA of iontophoretic current, as determined from the dose–response relationship) in both transgenic and wild-type neurons. Although we found no difference in decay time at day 10 or 14 *in vitro*, the decay time of the NMDA currents from transgenic neurons at day 18 was 1.8-fold longer than that of wild-type neurons (Fig. 2c, inset and Fig. 2e; $P < 0.005$). In addition, transgenic neurons retained the juvenile-like, single-synapse peak NMDA-current amplitude over time in culture. This is in contrast to that of wild-type neurons, which decreased significantly by day 18 *in vitro* (Fig. 2d, significance between NR2B ($n = 18$) and wild type ($n = 8$), $P < 0.01$; significance between day 14 ($n = 8$) and day 18 ($n = 8$) for wild type, $P < 0.01$). This indicates that the total number of NR2B-containing NMDA receptors per single synapse is also increased in transgenic neurons at this stage. These age-dependent changes in channel decay time and peak amplitude are consistent with the *in vivo* observation that the NR2B transgene messenger RNA was detectable but low at postnatal day 14 (P14), and gradually increased to steady level about one week later (data

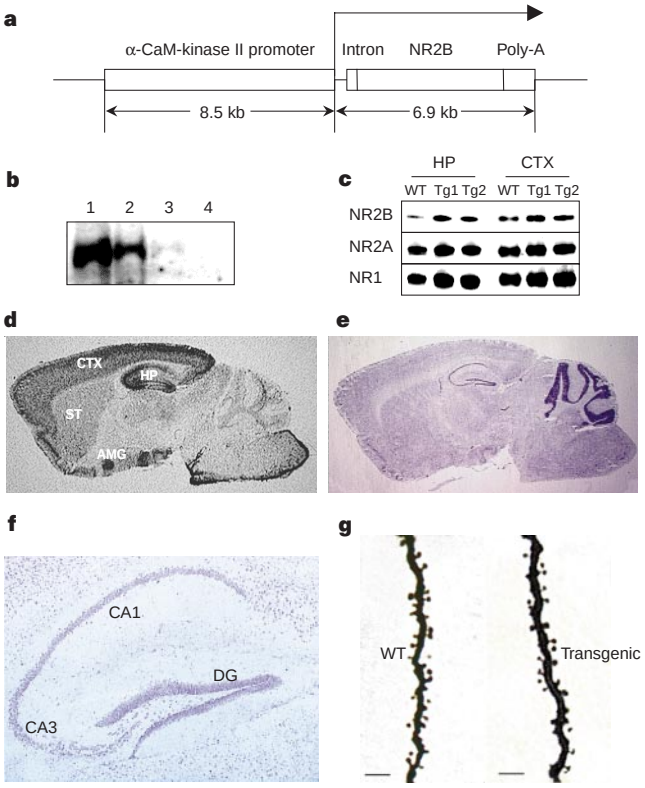

Figure 1 Construction and biochemical characterization of transgenic NR2B mice. **a**, The construct pJT–NR2B for production of NR2B transgenic mice. kb, kilobases. **b**, Expression of NR2B transgene mRNA in transgenic mice. Lane 1, cortex/striatum/amygdala; lane 2, hippocampus; lane 3, brain stem and thalamus; lane 4, cerebellum. **c**, Synaptic NMDA-receptor protein in hippocampus (HP) and cortex (CTX) in both transgenic lines (Tg-1 and Tg-2) and wild-type (WT). The same immunoblot was used for blotting with antibodies against NR1 (relative molecular mass 120K), NR2A (170K) and NR2B (180K). **d**, Forebrain-specific expression of NR2B transgene revealed by *in situ* hybridization. CTX, cortex; STM, striatum; HP, hippocampus; AMG, amygdala. **e**, Normal brain morphology in transgenic mice (Nissl staining). **f**, Higher magnification of the Nissl-stained transgenic hippocampus. DG, dentate gyrus; CA1 and CA3 are marked. **g**, Golgi staining of the dendritic spines of CA1 cells from wild-type (left) and transgenic mice (right). Scale bar, 5 μm.

not shown).

The prolonged decay time and the maintenance of a large single-synapse peak amplitude should result in increased charge transfer through the synaptic NMDA-receptor channel. We calculated the total amount of charge transfer associated with the activation of the NMDA receptors at a single synapse by integrating the area under the recorded current curve between the time of glutamate application and 400 ms later. The results clearly indicate that, at day 18 *in vitro*, the total charge transfer through single-synapse NMDA receptors was about 4-fold larger in transgenic mice than in controls (2.5 ± 0.7 pC ($n = 8$) in wild-type versus 9.8 ± 1.7 pC ($n = 18$) in NR2B mice, $P < 0.001$; Fig. 2f). Therefore, overexpression of the NR2B transgene results in prolonged opening of the NMDA receptors for detecting coincidence and enhanced NMDA activation in individual synapses, thus retaining several features of juvenile NMDA-receptor properties.

As blockade of the NMDA receptors prevents the induction of major forms of plasticity such as long-term potentiation and long-term depression (LTP and LTD)[2,3], we examined whether the increased window for coincidence detection by NMDA receptors leads to enhanced synaptic plasticity in the CA1 region of the hippocampus. Using hippocampal slices prepared from 4–6-month-old animals, we first measured (in blind fashion) NMDA-mediated field EPSPs in both adult wild-type and transgenic mice in the Schaffer collateral CA1 path. NMDA receptor-mediated EPSPs were isolated in the presence of 10 μM CNQX and 0.1 mM Mg^{2+}. NMDA-receptor-mediated field EPSPs in transgenic mice were significantly greater than those in wild-type mice, indicating that the overexpression of NR2B enhanced NMDA-receptor-mediated field responses (Fig. 3b). In addition, we confirmed that the observed synaptic responses were NMDA-receptor-dependent by showing that they were sensitive to the NMDA-receptor antagonist D(-)-amino-7-phosphonovaleric acid (AP5; 100 μM; $n = 3$; data not shown).

We then studied AMPA-receptor-mediated responses and found no difference in AMPA-mediated field EPSPs between transgenic mice ($n = 62$ slices/14 mice) and their wild-type littermates ($n = 50$ slices/16 mice, data not shown). Furthermore, paired-

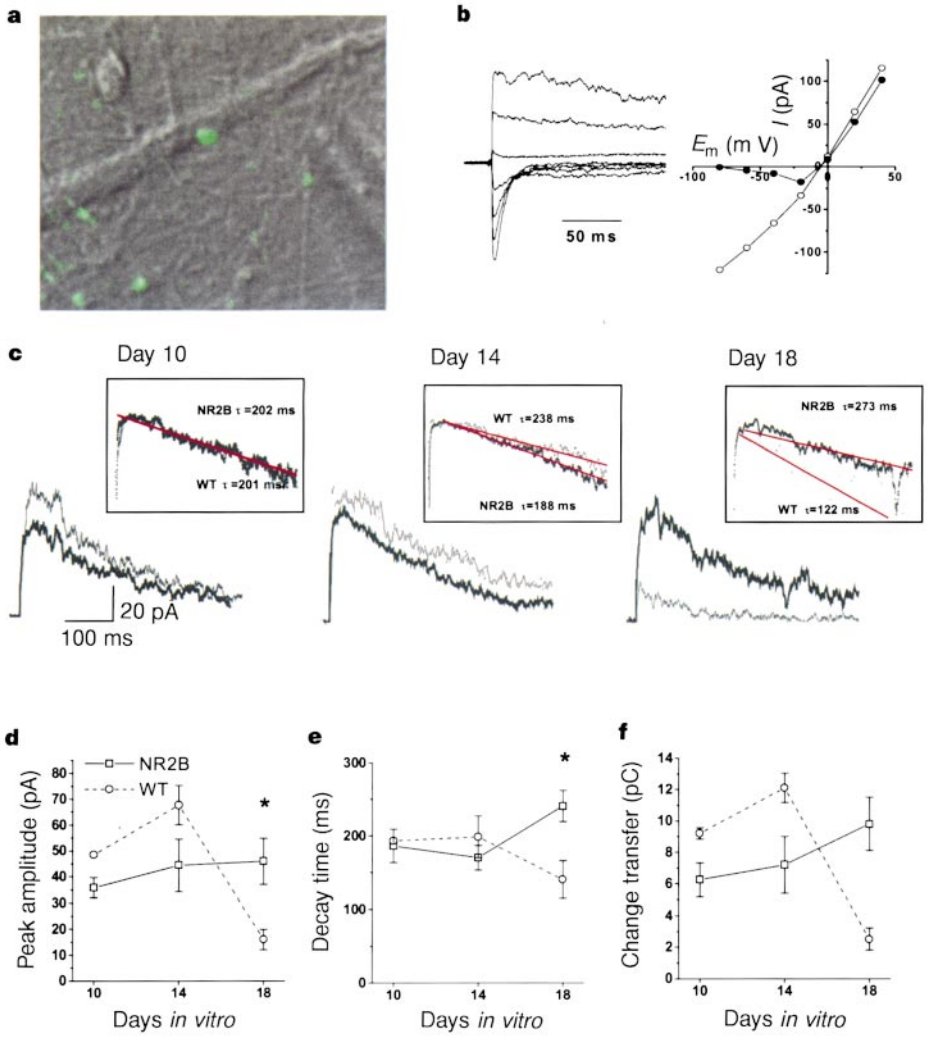

Figure 2 Developmental changes in NMDA current at single synapse. **a**, Confocal image of a dendrite with single synapses marked by FM 1-43 (green). The iontophoretic electrode on the right (out of the focal plan) was brought into close proximity to the FM spot to deliver glutamate (1 ms). **b**, Representative example of a current–voltage relationship of glutamate-evoked response from a single synapse from a wild-type neuron. At −80 to −40 mV, only non-NMDA current was observed, whereas at more positive potentials both non-NMDA (peak current typically observed at 3 ms after application) and NMDA current (peak current measured 30–40 ms after application) were recorded. The proportion of NMDA current evoked displays a typical 'J' shaped *I–V* relation (black circles) whereas non-NMDA current varies linearly with the membrane potential (open circles). **c**, Representative examples of NMDA currents at +40 mV recorded from WT (light trace) and transgenic mice (dark trace) at days 10, 14 and 18 *in vitro*, respectively. Insets display the same traces, normalized and expressed as a semi-log plot to emphasize the decay portion of NMDA currents. A single exponential, which provided excellent fits, was used to assess the decay time τ and values for the representative traces are indicated. **d**–**f**, Averaged values for peak amplitude, decay time and charge transfer of NMDA currents, respectively. Each point represents mean ± s.e.m. of 8–18 experiments obtained from 18 synapses on 13 neurons from 6 wild-type mice and 31 synapses on 19 neurons derived from 9 transgenic (Tg-1 and Tg-2 mice). Asterisks, significance between WT and transgenic mice ($P < 0.01$, 2-tailed unpaired Student's *t*-test).

pulse facilitation (PPF), which gives an indication of presynaptic function, was similar in transgenic ($n = 11$ slices/7 mice) and wild-type hippocampal slices ($n = 7$ slices/5 mice) (Fig. 3a). These results indicate that both presynaptic function and postsynaptic AMPA receptors are normal in transgenic animals.

To assess bidirectional synaptic plasticity in the 1–100 Hz range[18], we conducted a series of LTP/LTD experiments in the Schaffer collateral CA1 pathway in blind fashion. A single tetanic stimulation (100 Hz, 1 s) typically evoked smaller but reliable potentiation in 4–6-month-old control slices in comparison to that evoked in younger adult slices. However, the same stimulus evoked significantly larger potentiation in transgenic slices (Fig. 3c; transgenic, $n = 9$ slices/6 mice; wild-type, $n = 10$ slices/8 mice). The enhancement of potentiation was not due to changes in inhibitory GABA (γ-aminobutyric acid)-mediated mechanisms as it was also observed in the presence of 100 μM picrotoxin (transgenic, $n = 4$ slices/3 mice, mean $241.1 \pm 48.2\%$; wild-type, $n = 5$ slices/5 mice, mean $140.3 \pm 19.1\%$; $P < 0.05$ compared to transgenic mice). Moreover, the enhanced LTP was completely blocked by AP5 (100 μM; data not shown). In addition, in contrast to the normal fast decay of the field EPSP in control slices during the first 10 min after tetanic stimulation, there was no decay at all. Instead, it remained maximally potentiated, a feature resembling the juvenile LTP observed in postnatal day 15 animals[19].

Enhanced long-term potentiation in the transgenic slices was also observed when we applied prolonged, repetitive stimulation (10 Hz) to the Schaffer–CA1 path. Although 10-Hz stimulation for 1.5 min (900 pulses) did not induce reliable synaptic potentiation in wild-type animals ($n = 9$ slices/9 mice), it evoked robust synaptic potentiation in transgenic slices ($n = 5$ slices/5 mice) (Fig. 3d). However, repetitive stimulation delivered at 5 Hz for 3 min (also giving 900 pulses) did not produce significant synaptic potentiation in either group of mice (transgenic, $n = 5$ slices/5 mice; mean $96.8 \pm 20.3\%$; wild-type, $n = 5$ slices/5 mice, mean $85.0 \pm 16.4\%$).

We then investigated long-lasting synaptic depression induced by low-stimulation frequency[3,18]. Stimulation at 1 Hz produced similar LTD in both wild-type animals ($n = 6$ slices/6 mice, $76.0 \pm 9.3\%$) and transgenic mice ($n = 8$ slices/7 mice, $76.8 \pm 13.6\%$) (Fig. 3e). We also examined synaptic depression using another protocol in which low-frequency stimulation (5 Hz, 3 min) was applied 5 min after strong tetanic stimulation (100 Hz, 2×1 s)[20]. Again, similar depression or depotentiation was induced in slices from transgenic mice ($n = 4$ slices/4 mice; $129.3 \pm 12.9\%$) and wild-type mice ($n = 6$ slices/6 mice, $111.1 \pm 14.8\%$). Figure 3f summarizes our results, showing that enhanced NMDA-receptor activation in transgenic mice results in selective enhancement of long-lasting synaptic potentiation evoked by stimulation of 10–100 Hz.

How might the selective enhancement of 10–100-Hz LTP responses contribute to learning and memory? As forebrain neurons often fire in this frequency range during behavioural experience (for example, hippocampal neurons fire at 4–12 Hz, known as the θ-rhythm, whereas various cortical neurons oscillate at 20–60 Hz, known as the γ-frequency), it is possible that the selective enhancement of potentiation by stimuli at ⩾10 Hz in the transgenic mice is particularly meaningful. The conditional knockout of the NR1 subunit in the CA1 region leads to complete loss of synaptic changes

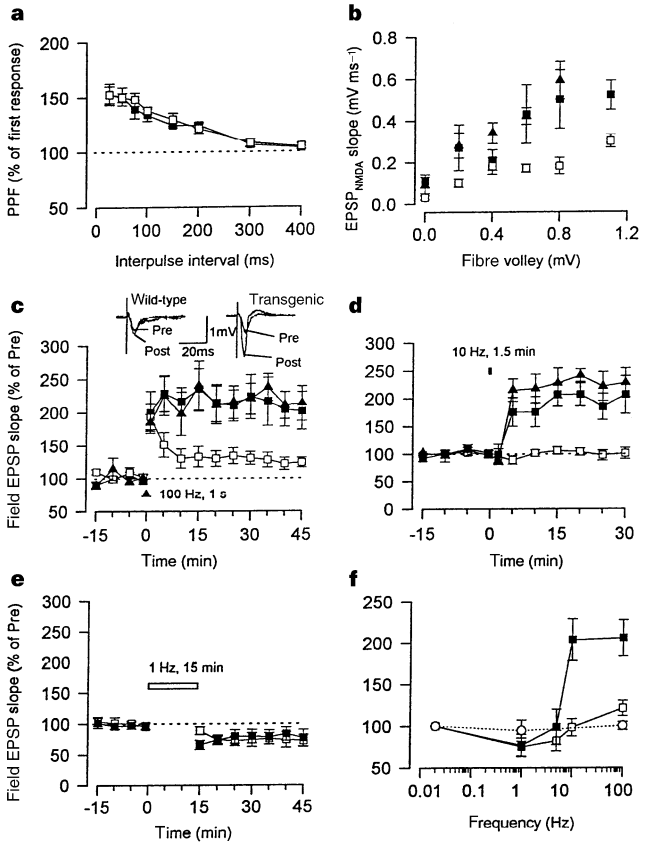

Figure 3 Selective enhancement of 10–100-Hz-induced potentiation in transgenic mice. Tg-1, filled squares; Tg-2, filled triangles; wild-type, open squares. **a**, Wild-type and transgenic mouse slices showed no significant difference in PPF of the EPSP at various interpulse intervals. **b**, Transgenic slices had larger NMDA-receptor-mediated EPSPs than wild-type slices. At 1.1 mV fibre volley, the area under the $EPSP_{NMDA}$ was 124.8 ± 20.6 (mV × ms) in transgenic mice and 31.1 ± 5.3 (mV × ms) in controls ($P < 0.001$). **c**, Tetanic stimulation (100 Hz, 1 s) induced significantly more potentiation in transgenic slices (Tg-1, 9 slices/6 mice; Tg-2, 6 slices/3 mice) than in wild-type slices ($n = 10$ slices/8 mice); Inset: representative records of the EPSP before (Pre) and 45 min after (Post) tetanus in a WT (left) and transgenic (right) slice. **d**, 10-Hz stimulation for 1.5 min produced significant synaptic potentiation in transgenic slices (Tg-1, 5 slices/5 mice; Tg-2, 4 slices/3 mice) but not WT slices (9 slices/9 mice). **e**, LTD induced by low-frequency stimulation (1 Hz for 15 min) is similar between WT and transgenic slices. **f**, Summary data for synaptic plasticity at different frequencies. For comparisons, results from our previous study of CA1-specific NR1 knockout mice (open circles, dotted line) is included.

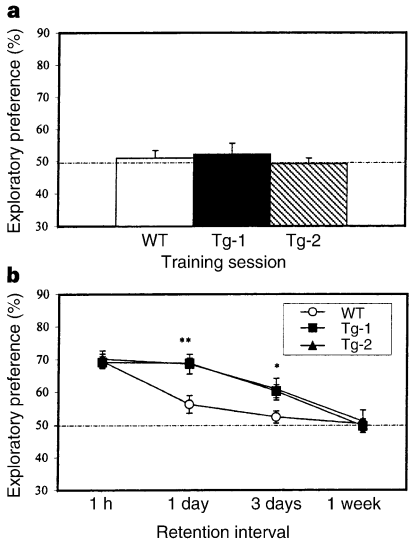

Figure 4 Enhanced novel-object recognition memory in transgenic mice. **a**, Exploratory preference in the training session. Dotted line represents performance at chance (50%). The amount of time spent exploring the two objects was the same for transgenic and wild-type mice. **b**, Enhanced exploratory preference in transgenic mice in retention test. Figure shows the temporary feature of the enhanced long-term memory in the transgenic mice (Tg-1, $n = 19$; Tg-2, $n = 8$; WT, $n = 14$). Data expressed as mean ± s.e.m. Single asterisk, $P < 0.05$; double asterisk, $P < 0.01$; *post hoc* analysis between transgenic and wild-type mice.

in the 1–100-Hz frequency range[21] (Fig. 3f) and impairs performance in a spatial water maze. This indicates that a normal frequency response in this range is essential for learning and memory. A systematic downward shift (producing LTD) in this specific range can cause learning impairment[15], whereas an upward shift (producing LTP) in all frequencies (1–100 Hz) is also deleterious to spatial learning[22]. These observations indicate the importance of normal 1–100-Hz responses for learning and memory.

To test whether the selective enhancement of responses to stimuli at 10–100 Hz represents an optimal plasticity curve, we conducted various learning tasks relevant to the forebrain regions. All behavioural experiments were performed with the experimenter blind to the genotype of each mouse.

We first used the novel-object-recognition task to measure visual recognition memory, which is evolutionarily conserved in species including humans and rodents and requires the hippocampus[23–25]. To increase the difficulty of this task, we used a 5-min training protocol (see Methods). During training there was no significant difference in the amount of the time the mice spent exploring the two novel objects (as shown by the exploratory preference; Fig. 4a), indicating that both types of mouse have the same curiosity and motivation to explore the objects. During the retention test one of the familiar objects used in the training session was replaced with a third novel object, and animals were allowed to explore for 5 min. Both transgenic and wild-type mice exhibited similar preference towards the novel object at the 1-h retention test (Fig. 4b). This indicates that all groups were equally able to retain the memory of the old object for 1 hour. However, when retention tests were conducted either 1 day or 3 days later (Fig. 4b), both transgenic lines exhibited much stronger preference for the novel object than did the wild-type mice ($F(2, 38) = 5.448$, $P < 0.01$), indicating that transgenic mice have better long-term memory. A *post hoc* analysis using Dunnett's test reveals a significant difference between wild-type and either transgenic line at the 1-day ($P < 0.01$) or 3-day retention tests ($P < 0.01$), but not between the two transgenic lines. The enhanced long-term memory is therefore independent of the transgene integration locus. However, by 1 week after training, the preference shown by transgenic mice also returned to the basal level.

We then assessed two forms of associative emotional memory in these mice: contextual and cued fear conditioning. Animals learn to fear either a neutral conditioned stimulus (such as tone) that has been paired with an aversive unconditioned stimulus (such as a foot shock) or a context in which the animals were conditioned by the pairing of conditioned and unconditioned stimuli. Contextual fear conditioning is hippocampus-dependent, whereas cued fear conditions is hippocampus-independent[26]. Both these types of fear conditioning require the activation of NMDA receptors[27,28].

Both contextual and cued conditioning were measured at 1 h, 1 day and 10 days after training using separate groups of animals. We first analysed contextual fear memory. Transgenic mice consistently exhibited much stronger freezing responses (Fig. 5a–c). One-way analysis of variance (ANOVA) indicated no significant difference in immediate freezing between wild-type and transgenic mice, but a significant group difference in contextual freezing is found when they are tested at 1 h ($F(2, 24) = 6.062$, $P < 0.05$), 1 day ($F(2, 25) = 5.223$, $P < 0.05$), and 10 days ($F(1.18) = 4.576$, $P < 0.05$). Further *post hoc* analysis reveals the significant difference between the wild-type and either transgenic line ($P < 0.05$, respectively), but not between these two transgenic lines.

As the transgene is also abundantly expressed in the amygdala and the cortex, we then examined cued fear conditioning. One-way ANOVA indicated that freezing in response to the tone was also significantly elevated in transgenic mice compared to that in controls when tested at 1 h ($F(2, 24) = 4.672$, $P < 0.05$), 1 day ($F(2, 25) = 5.518$, $P < 0.01$) or 10 days ($F(1.18) = 6.498$, $P < 0.05$) after training (Fig. 5d–f). A *post hoc* analysis shows the significant difference between wild-type and either transgenic line ($P < 0.05$, respectively). The enhanced contextual and cued fear memories in transgenic mice were not due to altered nociceptive responses, as the minimal amount of current required to elicit three stereotypical behaviours (flinching/running, jumping and vocalizing) were similar in wild-type and transgenic mice (data not shown).

We then conducted two experiments to measure emotional learning using the fear-extinction paradigm[29]. If animals are repeatedly exposed to the context or the conditioned stimulus (tone) without the unconditioned stimulus (shock), the context or conditioned stimulus will lose its ability to produce fear responses. This reduction in conditioned fear is known as fear extinction and is NMDA-dependent[29]. It is thought to involve the formation of a new

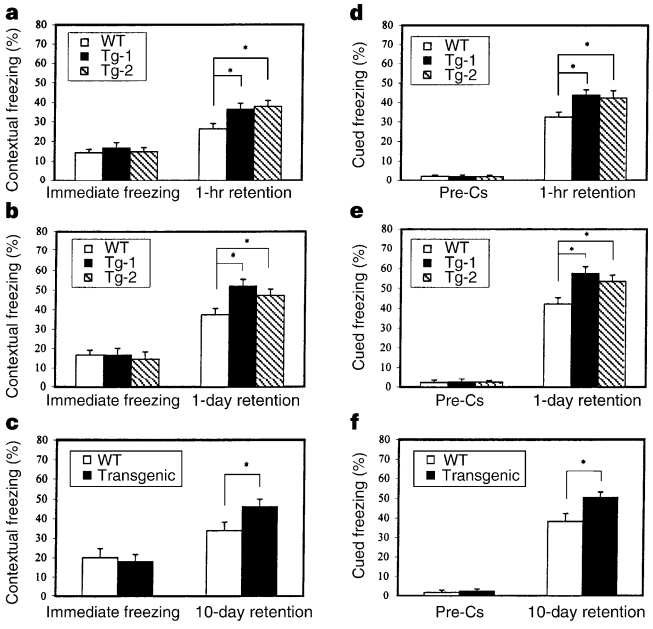

Figure 5 Enhancement of both contextual and cued fear memory in transgenic mice. **a**–**c**, Contextual conditioning 1 h, 1 day and 10 days after training, respectively. **d**–**f**, Cued fear conditioning 1 h, 1 day and 10 days after training, respectively. Each point represents data collected from 8–10 mice per group (WT, Tg-1 or Tg-2). The value in each column represents percentage of freezing rate and is expressed as mean ± s.e.m. Asterisk, $P < 0.05$, *post hoc* analysis between wild-type and transgenic mice.

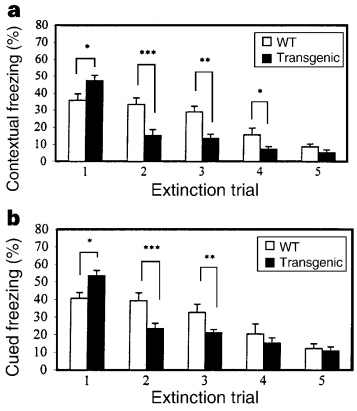

Figure 6 Transgenic mice exhibit faster learning in fear extinction. **a**, Faster fear extinction to contextual environment in transgenic mice. Either wild-type ($n = 8$) or transgenic (Tg-1, $n = 7$; Tg-2, $n = 8$; data plotted together) mice were given the same single CS/US pairing training as described in Fig. 5 and were then subjected to five extinction trials 24 h after training. **b**, Faster fear extinction to the tone in transgenic mice. The value in each column represents percentage of freezing rate; data are expressed as mean ± s.e.m. Asterisk, $P < 0.05$; double asterisk, $P < 0.01$; triple asterisk, $P < 0.001$, *post hoc* analysis.

memory rather than the passive decay or erasure of the original memory, because the original associations remain intact following extinction[29]. We examined fear extinction using a 5-extinction-trial protocol. When we measured the initial fear response 24 h after training, transgenic mice again showed much stronger fear responses than controls in both contextual and cued fear conditioning (Fig. 6). However, transgenic mice exhibited much less freezing during subsequent exposure to either the context or the tone than did wild-type mice (Fig. 6a, b). A two-way ANOVA indicated that, although both wild-type and transgenic mice decreased their freezing responses to contextual ($F(4, 80) = 86.247$, $P < 0.001$) or cued extinction ($F(4, 80) = 78.415$, $P < 0.001$), there was a significant group difference between transgenic and wild-type mice in contextual extinction ($F(2, 20) = 8.595$, $P < 0.01$) and in cued extinction ($F(2, 20) = 7.778$, $P < 0.01$). A *post hoc* analysis revealed a significant difference in the freezing responses between wild-type and transgenic mice at the second or third extinction trial in both contextual conditioning ($P < 0.05$) and cued conditioning ($P < 0.05$). Similar faster fear extinction was also observed if the experiments were conducted 1 h after fear conditioning (data not shown). Therefore, transgenic mice are quicker to learn to disassociate the previously paired events.

Finally, we tested spatial learning in transgenic mice using the hidden-platform water maze, which requires the activation of NMDA receptors in the hippocampus[21,30]. As shown in Fig. 7, the latency to escape to the platform in both wild-type and transgenic mice decreased following the training sessions. However, there was a significant group difference throughout sessions ($F(1, 26) = 9.655$, $P < 0.01$), indicating that spatial learning in transgenic mice was faster than in wild-type mice. Moreover, a *post hoc* analysis reveals a significant difference at the third session ($P < 0.05$), confirming better learning in transgenic mice. In addition, enhanced spatial learning in transgenic mice was also evident in the first transfer test conducted after the third training session. In comparison with controls, transgenic mice already exhibited a clear preference for the targeted quadrant in which the platform was previously located ($P < 0.05$; Student's *t*-tests) (Fig. 7b). With additional training, control mice showed the same preference as transgenic mice, as measured by either escape latency or place preference in the second transfer test after the last (sixth) session. Thus, the transgenic mice perform better than their wild-type littermates in this spatial task.

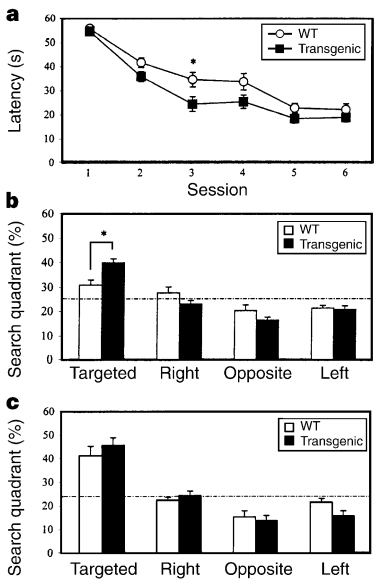

Figure 7 Enhanced performance in the hidden-platform water maze task by transgenic mice. **a**, Escape latency (mean ± s.e.m.) in water maze training (Tg-1, $n = 13$; wild-type, $n = 15$). **b**, Place preference in the first transfer test conducted at the end of the third training session. Transgenic mice spent more time in the target quadrant than other quadrants, whereas control mice did not show any preference for the target quadrant at this stage. **c**, Place preference in the second transfer test carried out at the end of the sixth training session. Both transgenic and wild-type mice exhibited strong preference for the target quadrant where the hidden platform was previously located. Asterisk, $P < 0.05$, *post hoc* analysis in **a**, and Student's *t*-test in **b**, between transgenic mice and controls.

We have shown that the NMDA receptor does serve as a graded molecular switch for gating the age-dependent threshold for synaptic plasticity and memory formation, thus substantially validating Hebb's learning rule. This further demonstrates that NMDA-dependent modifications of synaptic efficacy represent the unifying mechanism underlying a variety of associative learning and memory. Our data further indicate that neural activities at the 10–100 Hz range in the forebrain may be crucial for coding and storage of learned information. In addition, the identification of NR2B as a molecular switch in the memory process has indicated a potential new target for the treatment of learning and memory disorders. This study also reveals a promising strategy for the creation of other genetically modified mammals with enhanced intelligence and memory. □

Methods

For extended methods, see Supplementary Information.

Production and basic characterization of transgenic mice.

The transgenic founders were produced by pronuclear injection of the linearized DNA into C57B/6 inbred zygotes as described[16], and then intercrossed with B6/CBF1 for various analyses. F2 wild-type mice on this hybrid background consistently showed excellent learning. This mating strategy, therefore, sets a high standard for our behavioural enhancement experiments. For detailed procedures for genotyping, northern blot, western blot and *in situ* hybridization, see Supplementary Information.

Hippocampal cell culture and recording.

Primary cultures of hippocampal neurons were prepared from individual neonatal mice (P1). Whole-cell patch recordings were carried out as described[17]. Recordings were made with a 200B integrating patch-clamp amplifier (Axon Instruments) with a 1 kHz (8-pole Bessel) low-pass filter. Data were digitized at 10 kHz using a Digidata 1200B A/D converter (Axon Instruments). Glutamate currents were evoked by iontophoresis as described[17]. Briefly, following a one minute incubation in the FM 1-43 solution, neurons, continuously perfused with tyrode, were visualized under confocal microscopy. Following placement of the iontophoresis electrode, brief (1 ms) glutamate pulses of varied amplitudes were delivered to an isolated FM-labelled presynaptic bouton.

Hippocampal slice recording.

Transverse slices of the hippocampus from transgenic and wild-type littermates (4–6-months old) were rapidly prepared and maintained in an interface chamber. A bipolar tungsten stimulating electrode was placed in the stratum radiatum in the CA1 region and extracellular field potentials were recorded using a glass microelectrode (3–12 MΩ, filled with ACSF) also in the stratum radiatum. Test responses were elicited at 0.02 Hz. We also measured PPF of the response at various interpulse intervals (25–400 ms). Data are presented as mean ± s.e.m. One-way ANOVA (with Duncan's multiple range test for *post hoc* comparison) and Student's *t*-test were used for statistical analysis.

Behavioural tests.

Adult transgenic and wild-type mice (3–6-month-old littermates) were used throughout all behavioural tests. Unless stated otherwise, ANOVA and *post hoc* Dunnett's test were used to determine genotype effects on the behavioural responses.

Novel object recognition task.

Mice were individually habituated to an open-field box (20 × 20 × 10 high inches) for 3 days. During training sessions, two novel objects were placed into the open field and the animal was allowed to explore for 5 min. The time spent exploring each object was recorded. During retention tests, the animals were placed back into the same box, in which one of the familiar objects used during training was replaced by a novel object, and allowed to explore freely for 5 min. A preference index, a ratio of the amount of time spent exploring any one of the two objects (training session) or the novel one (retention session) over the total time spent exploring both objects, was used to measure recognition memory.

Fear conditioning task.

We used a fear conditioning shock chamber (10 × 10 × 15 inches high) and TruScan multi-parameter activity monitors (Coulbourn Instruments). The conditioned stimulus (CS) used was an 85dB sound at 2,800 Hz, and the unconditioned stimulus (US) was a continuous scrambled foot shock at 0.75 mA. After the CS/US pairing, the mice were allowed to stay in the chamber for another 30 s for measurement of immediate freezing. During the retention test, each mouse was placed back into the shock chamber and the

freezing response was recorded for 3 min (contextual conditioning). Subsequently, the mice were put into a novel chamber and monitored for 3 min before the onset of the tone (pre-CS). Immediately after that, a tone identical to the CS was delivered for 3 min and freezing responses were recorded (cued conditioning).

Fear extinction experiment.

Twenty-four hours after training, the mice were given the first extinction trial. Each extinction trial consisted of contextual and cued extinction. The mice were first put individually into the shock chamber and observed for 3 min in the absence of the US to measure contextual extinction. Then, the mice were transferred into a novel box for measurement of the pre-CS response for 3 min (in the absence of the tone), and subsequently of cued conditioning for 3 min in the presence of the training tone. Following this, the same four extinction trials were given at 2-h intervals and freezing responses were recorded.

Water maze task.

The water-maze apparatus is a circular pool (1.2 m in diameter). The procedure was essentially as described[21]. The training protocol consisted of six sessions (4 trials per session per day). The navigation of the mice was tracked by a videocamera, and the escape latency to the platform was recorded. In addition, we carried out two transfer tests. The first was done at the end of the third session and the second at the end of the last session. During the transfer test, the platform was removed and the mice were allowed to swim in the pool for 60 s. The time spent in each quadrant was recorded. Student's *t*-test was used to determine genotype effect on the spatial preference.

Received 9 February; accepted 14 June 1999.

1. Stevens, C. F. & Sullivan, J. Synaptic plasticity. *Curr. Biol.* **8,** R151–153 (1998).
2. Bliss, T. V. & Collingridge, G. L. A synaptic model of memory: long-term potentiation in the hippocampus. *Nature* **361,** 31–39 (1993).
3. Bear, M. F. & Malenka, R. C. Synaptic plasticity: LTP and LTD. *Curr. Opin. Neurobiol.* **4,** 389–399 (1994).
4. Bourne, H. R. & Nicoll, R. Molecular machines integrate coincident synaptic signals. *Cell* (suppl.) **72,** 65–75 (1993).
5. Nakanishi, S. Molecular diversity of glutamate receptors and implications for brain function. *Science* **258,** 597–603 (1992).
6. Hollmann, M. & Heinemann, S. Cloned glutamate receptors. *Annu. Rev. Neurosci.* **17,** 31–108 (1994).
7. Monyer, H. *et al.* Heteromeric NMDA receptors: molecular and functional distinction of subtypes. *Science* **256,** 1217–1221 (1992).
8. Monyer, H., Burnashev, N., Laurie, D. J., Sakmann, B. & Seeburg, P. H. Developmental and regional expression in the rat brain and functional properties of four NMDA receptors. *Neuron* **12,** 529–540 (1994).
9. Sheng, M., Cummings, J., Roldan, L. A., Yan, Y. N. & Yan, L. Y. Changing subunit composition of heteromeric NMDA receptors during development of rat cortex. *Nature* **368,** 144–147 (1994).
10. Okabe, S. *et al.* Hippocampal synaptic plasticity in mice overexpressing an embryonic subunit of the NMDA receptor. *J. Neurosci.* **18,** 4177–4188 (1998).
11. Carmignoto, G. & Vicini, S. Activity-dependent decrease in NMDA receptor responses during development of the visual cortex. *Science* **258,** 1007–1011 (1992).
12. Hestrin, S. Activation and desensitization of glutamate-activated channels mediating fast excitatory synaptic currents in the visual cortex. *Neuron* **9,** 991–999 (1992).
13. Kuhl, P. K. Learning and representation in speech and language. *Curr. Opin. Neurobiol.* **4,** 812–822 (1994).
14. Konishi, M. Birdsong for neurobiologists. *Neuron* **3,** 541–549 (1989).
15. Mayford, M., Wang, J., Kandel, E. R. & O'Dell, T. J. CaMKII regulates the frequency-response function of hippocampal synapses for the production of both LTD and LTP. *Cell* **81,** 891–904 (1995).
16. Tsien, J. Z. *et al.* Subregion- and cell type-restricted gene knockout in mouse brain. *Cell* **87,** 1317–1326 (1996).
17. Liu, G., Choi, S. & Tsien, R. W. Variability of neurotransmitter concentration and nonsaturation of postsynaptic AMPA receptors of synapses in hippocampal cultures and slices. *Neuron* **22,** 395–409 (1999).
18. Dudek, S. M. & Bear, B. F. Bidirectional long-term modification of synaptic effectiveness in the adult and immature hippocampus. *J. Neurosci.* **13,** 2910–2918 (1993).
19. Harris, K. M. & Teyler, T. J. Developmental onset of long-term potentiation in area CA1 of the rat hippocampus. *J. Physiol. (Lond.)* **346,** 27–48 (1984).
20. Stubli, U. & Chun, D. J. Factors regulating the reversibility of long-term potentiation. *J. Neurosci.* **16,** 853–860 (1996).
21. Tsien, J. Z., Huerta, P. T. & Tonegawa, S. The essential role of hippocampal CA1 NMDA receptor-dependent synaptic plasticity in spatial memory. *Cell* **87,** 1327–1338 (1996).
22. Migaud, M. *et al.* Enhanced long-term potentiation and impaired learning in mice with mutant postsynaptic density-95 protein. *Nature* **396,** 433–439 (1998).
23. Reed, J. M. & Squire, L. R. Impaired recognition memory in patients with lesions limited to the hippocampal formation. *Behav. Neurosci.* **111,** 667–675 (1997).
24. Myhrer, T. Exploratory behavior and reaction to novelty in rats with hippocampal perforant path systems disrupted. *Behav. Neurosci.* **102,** 356–362 (1988).
25. Mumby, D. G. *et al.* Ischemia-induced object-recognition defects in rats are attenuated by hippocampal ablation before or soon after ischemia. *Behav. Neurosci.* **110,** 266–281 (1996).
26. Phillips, R. G. & LeDoux, J. E. Differential contribution of amygdala and hippocampus to cued and contextual fear conditioning. *Behav. Neurosci.* **106,** 274–285 (1992).
27. Kim, J. J., Fanselow, M. S., DeCola, J. P. & Landeira-Fernandez, J. Selective impairment of long-term but not short-term conditional fear by the *N*-methyl-D-aspartate antagonist APV. *Behav. Neurosci.* **106,** 591–596 (1992).
28. Davis, M., Hitchcock, J. & Rosen, J. B. in *The Psychology of Learning and Memory* (ed. Bower, G. H.) (Academic, New York, 1987).
29. Falls, W. A., Miserendino, M. J. D. & Davis, M. Extinction of fear-potentiated startle: blockade by infusion of an NMDA antagonist into the amygdala. *J. Neurosci.* **12,** 854–863 (1992).
30. Morris, R. G., Garrud, P., Rawlins, J. N. & O'Keefe, J. Place navigation impaired in rats with hippocampal lesions. *Nature* **24,** 681–683 (1982).

Supplementary information is available on *Nature*'s World-Wide Web site (http://www.nature.com) or as paper copy from the London editorial office of *Nature*.

Acknowledgements

We thank G. Bracket and L. Antonucci and their staff for the maintenance of Princeton Mouse Facility, M. Mayford and E. Kandel for providing the CaMKII promoter, S. Tonegwa for support of J.R.T.'s early cloning work (1995) on plasmid p279NB from which pJT-NR2B is derived and D. Prout for secretarial assistance and proofreading. This work was supported by Princeton University, Beckman Foundation and NIH (J.Z.T.).

Correspondence and requests for materials should be addressed to J.Z.T. (e-mail: jtsien@molbio. princeton.edu).

Growth-cone attraction to netrin-1 is converted to repulsion by laminin-1

Veit H. Höpker*§, Derryck Shewan†§, Marc Tessier-Lavigne‡, Mu-ming Poo* & Christine Holt†

** Department of Biology, University of California at San Diego, La Jolla, California 92093-0357, USA*
† Department of Anatomy, University of Cambridge, Cambridge CB2 3DY, UK
‡ Howard Hughes Medical Institute, Departments of Anatomy, and Biochemistry and Biophysics, University of Califronia, San Francisco, California 94143-0452, USA
§ These authors contributed equally to this work.

Growing axons are guided by both diffusible and substrate-bound factors[1–3]. Growth cones of retinal neurons exhibit chemoattractive turning towards the diffusible factor netrin-1 *in vitro*[4] and are guided into the optic nerve head (ONH) by localized netrin-1 (ref. 5). Here we report that, in *Xenopus*, laminin-1 from the extracellular matrix (ECM), converts netrin-mediated attraction into repulsion. A soluble peptide fragment of laminin-1 (YIGSR) mimics this laminin-induced conversion. Low levels of cyclic AMP in growth cones also lead to the conversion of netrin-induced attraction into repulsion[6], and we show that the amount of cAMP decreases in the presence of laminin-1 or YIGSR, suggesting a possible mechanism for laminin's effect. At the netrin-1-rich ONH, where axons turn sharply to leave the eye, laminin-1 is confined to the retinal surface. Repulsion from the region in which laminin and netrin are coexpressed may help to drive axons into the region where only netrin is present, providing a mechanism for their escape from the retinal surface. Consistent with this idea, YIGSR peptides applied to the developing retina cause axons to be misdirected at the ONH. These findings indicate that ECM molecules not only promote axon outgrowth, but also modify the behaviour of growth cones in response to diffusible guidance cues.

The finding that growth cones rapidly turn away from netrin-1 when little cytosolic cAMP is present[6] suggested that coincident signals impinging on the same intracellular signalling pathway can influence the behaviour of growth cones *in vivo* as they navigate complex terrains. Because laminin-1 is abundant in the developing optic pathway and can promote axon outgrowth from retinal neurons[7–9], we investigated whether it can act as a coincident regulator of netrin-1-guided growth. When grown on glass, poly-D-lysine or fibronectin, *Xenopus* retinal growth cones consistently showed attractive turning in the presence of a netrin-1 gradient (Fig. 1a–d), mediated by the receptor Deleted in colorectal cancer (DCC)[4]. In contrast, when plated on poly-D-lysine coated with a low concentration of laminin-1 (1 $\mu g\,ml^{-1}$), retinal axons showed heterogeneous responses to the netrin-1 gradient, composed of either